On the validity of Stokes–Einstein–Debye relations for rotational diffusion in colloidal suspensions

Gijsberta H. Koenderink,*[a] Haiyan Zhang,[b] Dirk G. A. L. Aarts,[a] M. Pavlik Lettinga,[ac] Albert P. Philipse[a] and Gerhard Nägele[c]

[a] *Van't Hoff Laboratory, Debye Institute, Utrecht University, 3584 CH, Utrecht, The Netherlands. E-mail: g.h.koenderink@chem.uu.nl*

[b] *Department of Physics, Shanghai Jiao Tong University, Shanghai 200030, P. R. China*

[c] *Institut für Festkörperforschung, Weiche Materie, Forschungszentrum Jülich, D-52425, Jülich, Germany*

Received 14th May 2002, Accepted 10th June 2002
First published as an Advance Article on the web 20th September 2002

According to the Stokes–Einstein–Debye (SED) relation, the rotational diffusion coefficient of a colloidal tracer sphere scales with the inverse of the solvent viscosity. Here we investigate the generalization of the SED relation to tracer diffusion in suspensions of neutral and charged colloidal host spheres. Rotational diffusion coefficients are measured with dynamic light scattering and phosphorescence spectroscopy, and calculated including two- and three-particle hydrodynamic interactions. We find that rotational tracer diffusion is always faster than predicted by the SED relation, except for large tracer/host size ratios λ. In the case of neutral particles this observation is rationalized by introducing an apparent λ-dependent slip boundary coefficient. For charged spheres at low ionic strength, large deviations from SED scaling are found due to the strongly hindered host sphere dynamics. Finally, we present some first experiments on tracer sphere diffusion in suspensions of host rods, showing that hydrodynamic hindrance by rods is much stronger than by spheres. We conclude by pointing to some interesting unresolved issues for future research.

I Introduction

The rotational diffusion coefficient of a single colloidal sphere with radius a_T suspended in a solvent with shear viscosity η_0 is given by the familiar Stokes–Einstein–Debye (SED) relation[1–3]

$$D_0^r = \frac{k_B T}{f_0^r} = \frac{k_B T}{8\pi\eta_0 a_T^3} \tag{1}$$

with $k_B T$ the thermal energy and f_0^r the Stokesian friction factor. Eqn. (1) assumes that the particle is large enough for the solvent to behave as a structureless continuum with vanishing response time. Moreover, stick boundary conditions are assumed, *i.e.* the velocity of the fluid on the tracer surface equals that of the tracer. Eqn. (1) holds quantitatively not only for colloidal particles but,

surprisingly, also for many molecular solutes, in particular when the numerical prefactor 8 (no slip) in f_0^r is changed to a value close to zero (complete slip).[4–7]

An interesting question is whether eqn. (1) can be generalized to the case of a colloidal tracer in a colloidal host fluid, with η_0 replaced by the higher viscosity of the host suspension. A practical motivation for studying this issue is that a generalized SED relation would allow one to extract rheological properties of a suspension from the rotational dynamics of a dispersed tracer particle. In contrast to conventional rheology, such a microrheological[8,9] experiment employs small sample volumes, is noninvasive, and allows one to measure local viscosities in inhomogeneous (biological) samples. However, as for molecular diffusion, the continuum assumption underlying eqn. (1) is expected to break down unless the tracer/host sphere size ratio $\lambda = a_T/a_H$ is very large. In addition, the rotational dynamics will split into a short- and long-time regime due to hydrodynamic interactions (HI) and direct interactions (DI) between the colloids. To distinguish between short and long times one can define the interaction time scale

$$\tau_0^I = \frac{a_T^2}{D_0^t} \tag{2}$$

which is the time roughly required for a significant change in the suspension microstructure. Here, D_0^t is the Stokesian translational diffusion coefficient of a single tracer sphere (see eqn. (4) below). For identical tracer and host spheres ($\lambda = 1$) the structural relaxation time $\tau_0^I = 3/(4D_0^r)$ is of the same order of magnitude as the rotational diffusion time $(D_0^r)^{-1}$. In the short-time regime $t \ll \tau_0^I$, the tracer particle slightly rotates in an essentially static configuration of neighboring particles, so its short-time self-diffusion coefficient D_s^r with $D_s^r \leqslant D_0^r$ is a hydrodynamic quantity controlled by HI averaged over the equilibrium configuration.[10–16] At long times $t \gg \tau_0^I$, the tracer experiences many realizations of host-particle configurations so now DI affect diffusion directly through memory effects, *i.e.* sphere caging. As a result, the long-time diffusion coefficient D_L^r is smaller than D_s^r.[17] We note that for tracer/host size ratios $\lambda \gg 1$ the small host particles diffuse (much) faster than the tracer particle, so that "short-time" implies times $t \ll \tau_0^I/\lambda^2$. The separation of time scales suggests the following generalization of eqn. (1):

$$D_s^r(\phi) = \frac{k_B T}{8\pi\eta_\infty(\phi)a_T^3}(t \ll \tau_0^I) \text{ and } D_L^r(\phi) = \frac{k_B T}{8\pi\eta_L(\phi)a_T^3}(t \gg \tau_0^I). \tag{3}$$

Here ϕ is the volume fraction of the host fluid, with a high frequency limiting viscosity η_∞ and a low-shear viscosity η_L. D_s^r and η_∞ are both hydrodynamic quantities, while D_L^r and $\eta_L > \eta_\infty$ are long-time transport coefficients in a dispersion slightly disturbed from equilibrium by, respectively, the diffusing tracer or an external flow.

The translational diffusion coefficient of a tracer sphere in a colloidal fluid at infinite dilution is given by the Stokes–Einstein (SE) relation[1,2]

$$D_0^t = \frac{k_B T}{f_0^t} = \frac{k_B T}{6\pi\eta_0 a_T}, \tag{4}$$

where f_0^t is the Stokesian friction factor for stick boundary conditions. In the case of perfect slip, where friction is due only to the solvent displaced by the diffusing tracer, $f_0^t = 4\pi\eta_0 a_T$. Generalizations of eqn. (4) to finite host concentrations,

$$D_s^t(\phi) = \frac{k_B T}{6\pi\eta_\infty(\phi)a_T}(t \ll \tau_0^I) \text{ and } D_L^t(\phi) = \frac{k_B T}{6\pi\eta_L(\phi)a_T}(t \gg \tau_0^I), \tag{5}$$

have been proposed, *e.g.* in ref. 18, in complete analogy to eqn. (3), introducing the short-time, D_s^t, and long-time, D_L^t, translational tracer diffusion coefficients with $D_0^t \geqslant D_s^t > D_L^t$. The validity of eqn. (5) has been tested for monodisperse suspensions of identical host and tracer particles. At long times $t \gg \tau_0^I$, eqn. (5) holds fairly well for colloidal hard spheres,[19–21] but theory[18,22] predicts that it fails in the case of charged sphere suspensions with low electrolyte concentrations. At short times $t \ll \tau_0^I$, deviations from eqn. (5) have been observed both for neutral and charged spheres.[18,23]

Up to now, no systematic analysis has been performed of the accuracy of the SED relations for rotational diffusion in eqn. (3). Experimental studies of rotational diffusion in dense sphere suspensions are scarce, since special labelled colloids are required. The volume fraction dependence of short-time rotational diffusion of monodisperse hard-spheres up to the freezing transition volume fraction $\phi = 0.49$ has now been measured by various groups.[11,14,24] Recently, we have also measured[14,25,26] and calculated[14] rotational diffusion of charged spheres in binary colloidal mixtures.

In this paper we investigate, both by experiment and theory, the applicability of SED scaling to rotational diffusion of tracer spheres in colloidal host suspensions according to eqn. (3). Our expectation is that eqn. (3) (and eqn. (5)) will hold for sufficiently large tracers (large size ratio λ) in a host fluid with sufficiently fast dynamics. We study the influence of several factors which control the host dynamics, namely the host density ϕ, the ionic strength and host particle charge, and the host particle shape (*i.e.* thin rods *vs.* spheres). It is shown that SED scaling fails, except in the continuum limit, where the tracer is much larger than the host particles. However, modified versions of eqn. (3), assuming slip boundary conditions for the host spheres on the tracer surface, are in fair agreement with measured and calculated rotational diffusion coefficients.

II Theory

We have calculated the reduced short-time rotational diffusion coefficient $H_s^r = D_s^r/D_0^r$ of a single tracer sphere in host sphere suspensions of charged and neutral spheres, for variable tracer/host size ratio $\lambda = a_T/a_H$ and host volume fraction ϕ (*cf.* ref. 14 and 16). Our calculation is a generalization of earlier work on monodisperse hard-sphere suspensions.[10,13]

For small to moderate values of ϕ, H_s^r can be approximately calculated using a truncated rooted cluster expansion, involving hydrodynamic interactions (HI) between clusters consisting of a tracer with one and two host spheres, according to:

$$H_s^r(\phi,\lambda) \approx 1 + H_{s1}^r(\phi,\lambda)\phi + H_{s2}^r(\phi,\lambda)\phi^2. \tag{6}$$

The two-body coefficient $H_{s1}^r(\phi,\lambda)$ can be expressed in terms of the integral

$$H_{s1}^r(\phi,\lambda) = \frac{1}{a_H^3}\int_{a_H+a_T}^{\infty} \mathrm{d}r\, r^2 g_{TH}^{(2)}(r;\phi,\lambda)[\alpha_{TH}^{rr}(r;\lambda) + 2\beta_{TH}^{rr}(r;\lambda)], \tag{7}$$

involving the tracer–host radial distribution function $g_{TH}^{(2)}(r;\phi,\lambda)$, and the two-body hydrodynamic mobility functions $\alpha_{TH}^{rr}(r;\lambda)$ and $\beta_{TH}^{rr}(r;\lambda)$ which depend on λ and on the tracer–host particle distance r. For $\lambda = 1$, multipole expansions of these mobility functions in powers of r^{-1} are known, in principle, to arbitrary order.[10,13] For $\lambda \neq 1$, explicit r^{-1}-expansions including contributions up to $O(r^{-12})$, are available.[27,28] To calculate the three-body coefficient $H_{s2}^r(\phi,\lambda)$ for $\lambda \neq 1$, we have used the method of reflections and connectors to derive the leading order r^{-9} term of the three-body mobility tensor.[16] Using this asymptotic form, $H_{s2}^r(\phi,\lambda)$ is given by a threefold integral,

$$H_{s2}^r(\phi,\lambda) = \frac{225}{16}\phi^2\left(\frac{\lambda}{1+\lambda}\right)^3 \int_0^1 \mathrm{d}t_{12} \int_0^1 \mathrm{d}t_{13} \int_{-1}^1 \mathrm{d}\xi_1 g_{THH}^{(3)}(t_{12},t_{13},\xi_1)\frac{(t_{12}t_{13})^2}{h^{3/2}} f(t_{12},t_{13},\xi_1), \tag{8a}$$

with

$$f(t_{12},t_{13},\xi_1) = \frac{t_{12}t_{13}\xi_1(1-\xi_1^2)}{h} + \xi_1^2 - 1 - \frac{2}{h^2}(t_{12} - t_{13}\xi_1)(t_{13} - t_{12}\xi_1) \times \left[(t_{12}^2 + t_{13}^2)\xi_1 - t_{12}t_{13}(5 - 3\xi_1^2)\right] \tag{8b}$$

over the static triplet distribution function $g_{THH}^{(3)}$. The latter describes static correlations between a tracer and two host spheres as a function of the reduced distances $t_{1i} = (a_T + a_H)/r_{1i}$ and the

angular cosine $\xi_1 = \vec{r}_{12} \cdot \vec{r}_{13}/(r_{12}r_{13})$, where $\vec{r}_{1i} = \vec{r}_1 - \vec{r}_i$ is the vector pointing from host particle i to the tracer 1 (and $r_{1i} = |\vec{r}_{1i}|$), and $h = t_{12}^2 + t_{13}^2 - 2\xi_1 t_{12} t_{13}$. Eqns. (8a) and (8b) reduce to the asymptotic three-body result of Cichocki *et al.*[13] for $\lambda = 1$.

For neutral tracer and host spheres, a virial expansion up to quadratic order in ϕ, *viz.*

$$H_s^r(\phi,\lambda) = 1 + h_1^r(\lambda)\phi + h_2^r(\lambda)\phi^2, \tag{9}$$

can be deduced from eqn. (6). To obtain eqn. (9) we have substituted the leading-order in ϕ form

$$g_{TH}^{(2)}(x) = \{1 + \phi f(x,\lambda)\Theta([3+\lambda] - x) + O(\phi^2)\}\Theta(x - [1+\lambda]) \tag{10}$$

for $g_{TH}^{(2)}$, where $x = r/a_H$, Θ is the unit step function, and $f(x,\lambda)$ is an overlap function.[16] For $g_{THH}^{(3)}$ we have employed the zero-density form $g_{THH}^{(3)} = \Theta(r_{12} - [a_T + a_H])\Theta(r_{13} - [a_T + a_H])\Theta(r_{23} - 2a_H)$.

Since charged colloids are strongly correlated even at small ϕ, calculations of $g_{TH}^{(2)}$ and $g_{THH}^{(3)}$ are more involved than for hard spheres. Instead of virial expansions, we use the Rogers–Young (RY) integral equation scheme[29] to compute the radial distribution functions. The effective pair potential between two charged colloidal spheres is modeled as a sum of a hard-sphere part and a screened DLVO-type potential $V(r)$.[12] Assuming constant colloidal surface charges Z_T and Z_H of tracer and host spheres,[12,14] $V(r)$ reads

$$V(r) = \frac{Z_T Z_H e^2}{4\pi\varepsilon} \frac{\exp(\kappa[a_T + a_H])}{(1+\kappa a_T)(1+\kappa a_H)} \frac{\exp(-\kappa r)}{r} \tag{11}$$

for the tracer–host effective electrostatic interactions, with e the elementary charge, ε the solvent dielectric constant, and κ^{-1} the Debye screening length. For $g_{THH}^{(3)}$ we use Kirkwood's superposition approximation $g_{THH}^{(3)} \approx g_{TH}^{(2)}(r_{12}) g_{TH}^{(2)}(r_{13}) g_{HH}^{(2)}(r_{23})$, where $g_{HH}^{(2)}$ is the pair distribution function for two host spheres. HI are more easily accounted for when the colloidal spheres are charged since $g_{TH}^{(2)}$ is then practically zero for small distances r. Thus, only the leading far-field terms of the mobility functions are needed in the expressions for H_{s1}^r and H_{s2}^r.

For comparison with rotational diffusion, we also include theoretical results for the translational short-time tracer diffusion coefficient $H_s^t(\phi,\lambda)$ using the same approximate scheme as for rotational diffusion. Details of these involved calculations are given elsewhere.[10,13]

We remark that our theoretical approach for calculating $H_s^r(\phi,\lambda)$ and $H_s^t(\phi,\lambda)$ is suitable only for values of λ not far from unity, with the applicable ϕ-range becoming smaller for increasing size asymmetry.

III Experimental methods

Rotational diffusion coefficients have been measured in binary dispersions of negatively charged tracer and host particles using two techniques, namely time-resolved phosphorescence anisotropy (TPA) for binary sphere mixtures with $\lambda = 0.2$–1 (partly discussed elsewhere)[14,26] and for sphere–rod mixtures, and depolarized dynamic light scattering (DDLS) for binary sphere mixtures with $\lambda = 10$.[25]

TPA was applied to tracer spheres (*cf.* Table 1, Fig. 1A and B), covalently labeled with eosin-5-isothiocyanate. The rotational tracer diffusion coefficient D_s^r follows from the decay rate of the polarization anisotropy measured after excitation of the phosphorescent dye with a vertically polarized laser light pulse.[14,26,30] The experimentally accessible time scale is limited by the lifetime of the excited state of the dye to about 10 ms. Host particles are silica spheres (Table 1, Fig. 1C), and rods prepared by coating boehmite (γ-AlOOH) cores with a 4.5 nm thick silica layer[31] (Fig. 1D). The average length and diameter of the rods determined from electron microscopy are 203 ± 93 nm and 18 ± 3 nm respectively. The silica spheres were dispersed in a mixture of dimethylsulfoxide-*N*,*N*-dimethylformamide (3:2 v/v DMSO–DMF), while the rods were dispersed in DMF. In both cases, LiCl was added to adjust the ionic strength. Both the spheres and the rods are stable up to high LiCl concentrations ($\sim$400 mM) due to their surface charges, the weakness of the van der Waals attractions, and strong solvation.[26]

DDLS was performed on fluorocarbon tracer spheres (PFA, Ausimont) dispersed in aqueous suspensions of silica host spheres (Ludox AS-40, DuPont) with variable amounts of added NaCl.

Table 1 Parameters of experimentally studied tracer sphere–host sphere suspensions (PFA = perfluoroalkylvinylether, PS = polystyrene, Ludox is a trade name for silica (DuPont), other names refer to synthesis products). Listed are the tracer and host particle radii a_T and a_H (in nm) with relative size polydispersity σ, size ratio $\lambda = a_T/a_H$, and estimates for the apparent slip parameter $\nu_s^r(\text{exp})$. The latter is determined experimentally in the hard-sphere-like regime of high salt concentration, by averaging the $\nu_s^r(\phi,\lambda)$ deduced from eqn. (20) over the ϕ-range $0 < \nu_s^r(\phi) < 0.45$, with the experimental $H_s^r(\phi,\lambda)$ as input. Further included is the zero-ϕ limit $\nu_s^r(\lambda,\phi \to 0)$ of hard spheres according to eqn. (19)

System	$a_T(\sigma)$	$a_H(\sigma)$	λ	$\nu_s^r(\text{exp})$	$\nu_s^r(\lambda,\phi \to 0)$
μ10-SC_{08}	72 (2%)	298 (2%)	0.24[a]	0.071	0.030
eR75-SC_{08}	95 (9%)	298 (2%)	0.32[a]	0.089	0.049
μ10-SC_{07}	72 (2%)	217 (2%)	0.33[a]	0.080	0.051
μ30-SC_{08}	100 (3%)	298 (2%)	0.34[a]	0.089	0.054
μ30-SC_{07}	100 (3%)	217 (2%)	0.46[a]	0.127	0.084
μ10-R75	72 (2%)	93 (8%)	0.76[a]	0.250	0.155
eR75-R75	95 (9%)	93 (8%)	1.00[a]	0.188	0.252
PFA-PFA	110 (2%)	110 (2%)	1.00[b]	0.226	0.252
PS-PS	219 (13%)	219 (13%)	1.00[c]	0.224	0.252
PFA-Ludox	93 (10%)	9.0 (20%)	10.3[d]	1.49	0.76

[a] Solvent DMSO–DMF (3:2 v/v) with 100 mM LiCl; technique TPA. [b] Solvent water–urea (4:1 w/w) with 100 mM NaCl; technique DDLS. [c] Solvent water–glycerol (4:1 w/w) with no added salt; technique NMR. [d] Solvent water with 10 mM NaCl; technique DDLS.

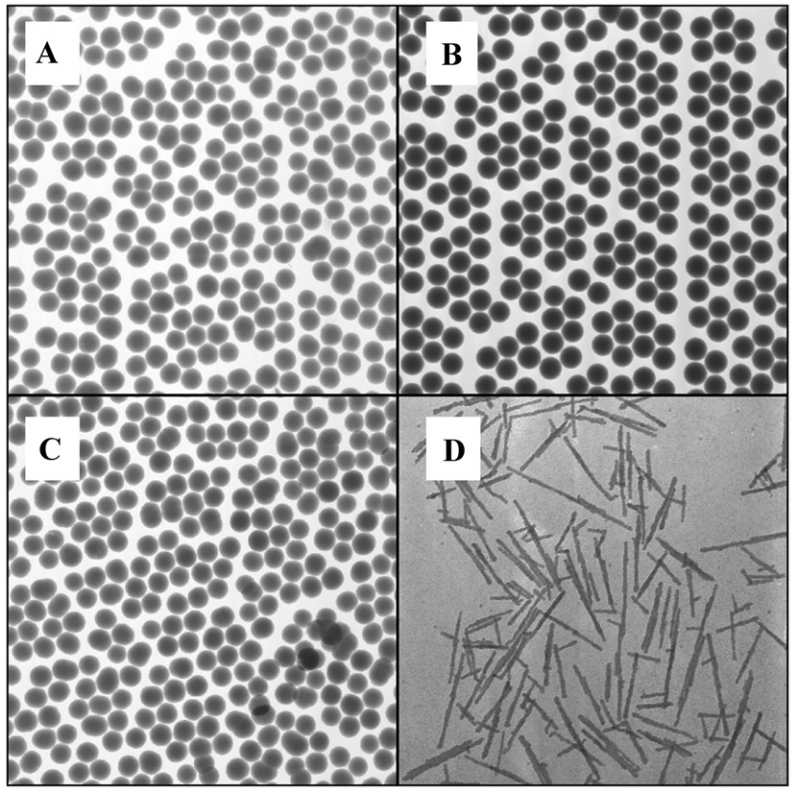

Fig. 1 Transmission electron microscopy (TEM) pictures of eosin-labeled silica tracer spheres denoted as A: eR75 and B: μ30, unlabeled host silica spheres denoted as C: R75 (*cf.* Table 1), and D: silica-covered boehmite host rods.

The mixtures are stable up to NaCl concentrations of 10 mM, but flocculate in the presence of 100 mM NaCl, probably due to depletion attraction between the large particles induced by the small ones. (The separate PFA and Ludox dispersions are stable in the presence of 100 mM added NaCl.) DDLS measurements were performed using a vertically polarized argon laser at 514.5 nm. The experiment exploits the fact that the PFA particles, by virtue of their partially crystalline internal structure, significantly depolarize light. The horizontally polarized scattered intensity was measured in the horizontal scattering plane. In all cases, the full shape of the intensity autocorrelation functions $g_{VH}(t)$ was a single exponential given by $g_{VH}(t) \propto \exp\{-2(6D^r + q^2D^t)t\}$, where q denotes the wave number.

Measurements of the zero-shear-limiting ("long-time") viscosity η_L were made on 1 mL samples using a Contraves Low Shear 40 rheometer. A measurement of the high-frequency-limiting viscosity η_∞ typically requires large sample volumes ($\geqslant$20 mL), which were unfortunately not available due to the small scale of our model-colloid synthesis. Therefore, for hard-sphere-like dispersions we use a semi-empirical expression for η_∞ due to Lionberger and Russel,[32] *i.e.*

$$\frac{\eta_\infty}{\eta_0} = \frac{1 + \frac{3}{2}\phi(1 + \phi - 0.189\phi^2)}{1 - \phi(1 + \phi - 0.189\phi^2)}, \tag{12}$$

which agrees well with known experimental data up to random close packing, where η_∞ diverges. For dilute suspensions of highly charged host spheres at low ionic strength, only pair-wise additive far-field HI need to be accounted for, so that to a good approximation

$$\eta_\infty/\eta_0 \approx 1 + \frac{5}{2}\phi(1 + \phi) + \frac{15}{2}\phi^2 \int_0^\infty \mathrm{d}x x^2 g_{HH}^{(2)}(x) J(x), \tag{13}$$

with $J(x) \approx (15/2)x^{-6}$ for $x = r/a_H \gg 1$. Using an effective hard-sphere model for $g_{HH}^{(2)}(r)$, eqn. (13) can be further approximated by[18]

$$\eta_\infty/\eta_0 \approx 1 + \frac{5}{2}\phi(1 + \phi) + 7.9\phi^3, \tag{14}$$

which is practically equal to the Einstein result $1 + (5/2)\phi$ for $\phi < 0.1$. We are not aware of any closed analytical expressions for $\eta_\infty(\phi)/\eta_0$ of charged spheres with stronger screening of the electrostatic double layer repulsions. The few measurements available[22,33,34] suggest, however, that $\eta_\infty(\phi)/\eta_0$ is only weakly dependent on κ^{-1}.

IV SED scaling in monodisperse hard-sphere suspensions

First we focus on SED scaling for the most extensively studied case of monodisperse colloidal hard spheres (*i.e.* $\lambda = 1$). This section is split into a section on short-time rotational tracer diffusion (where both calculations and experiments have been performed) and a section on long-time tracer diffusion.

IVa Short-time rotational tracer diffusion

The most accurate truncated virial expansion calculation of the reduced short-time rotational diffusion coefficient $H_s^r(\phi)$ of hard spheres up to quadratic order in ϕ was performed by Cichocki *et al.*[13] These authors account for short-range lubrication interactions, and for expansions of the two- and three-body mobility functions up to $O(r^{-1000})$ and $O(r^{-21})$ respectively. Their result reads

$$H_s^r \approx 1 - 0.6310\phi - 0.726\phi^2. \tag{15}$$

This second order virial form agrees well with simulation results[35,36] (*cf.* inset of Fig. 2). The excellent agreement at high densities is most likely fortuitous, regarding the severe low-density approximations used for $g_{TH}^{(2)}$ and $g_{THH}^{(3)}$ in deriving eqn. (15). In Fig. 2 we compare eqn. (15) with our TPA data for silica spheres in DMSO–DMF with 100 mM added LiCl (at $\kappa a_H = 126$), DDLS data for PFA spheres in water–urea solvent mixtures of Degiorgio *et al.*,[11] and nuclear magnetic

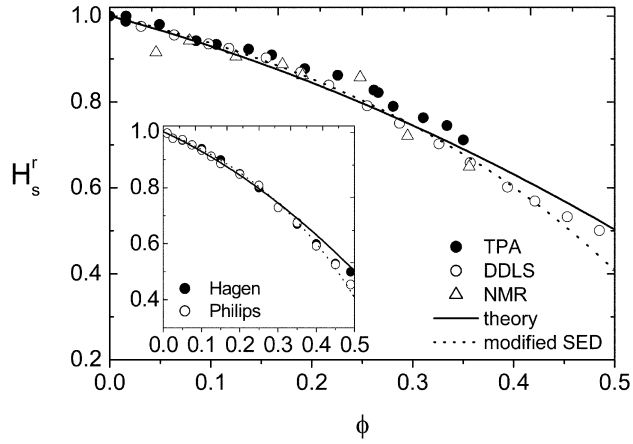

Fig. 2 Reduced short-time rotational diffusion coefficient $H_s^r = D_s^r/D_0^r$ of monodisperse hard-sphere suspensions, including experimental results,[14,26] the theoretical virial expression eqn. (15), and the modified SED result eqn. (18), with η_∞/η_0 as in eqn. (12) and $\nu_s^r = 0.22$ (partial slip). The inset includes a comparison between eqn. (15), simulation data of Philips *et al.*[35] and of Hagen *et al.*,[36] and the modified SED prediction for H_s^r.

resonance (NMR) data for polystyrene latex spheres in water–glycerol of Kanetakis *et al.*[37] (*cf.* Table 1). All these experimental data are in fair agreement with each other and with eqn. (15). It should be noted that all experiments were done with charged particle suspensions with highly screened double layers. To our knowledge no experiments have been performed on suspensions of uncharged particles. The deviations between the experimental data and eqn. (15) can thus be at least partially attributed to residual double layer repulsions. Moreover, it is well known that silica spheres in DMF are strongly solvated.[26] Calculations have revealed that H_s^r is indeed highly sensitive to the shape of the static pair distribution function $g_{TH}^{(2)}(r)$ near contact.[12]

A convenient graphical method to check the validity of SED scaling for D_s^r is to plot $H_s^r\eta_\infty/\eta_0$ *versus* ϕ. If SED scaling holds, the product is equal to one (*cf.* eqns. (1) and (3)). Fig. 3 shows results for $H_s^r\eta_\infty/\eta_0$ assembled from the experimental H_s^r results depicted in Fig. 2, and with η_∞/η_0 according to eqn. (12). The experimental data are in good overall agreement, for $\phi \leqslant 0.4$, with the theoretical prediction (drawn line) obtained by multiplying eqn. (15) for H_s^r with eqn. (12) for η_∞/η_0. Clearly, the short-time SED relation eqn. (3) for D_s^r does not hold at finite host concentrations.

For comparison, Fig. 3 displays in addition results for the SE product $H_s^t\eta_\infty/\eta_0$ of the reduced *translational* short-time self-diffusion coefficient H_s^t of hard spheres with η_∞/η_0 according to eqn. (12). For H_s^t, we use DDLS results of Degiorgio *et al.*,[11] DLS results of Segrè *et al.*,[38] and the semi-empirical formula

$$H_s^t = (1 - 1.56\phi)(1 - 0.27\phi). \tag{16}$$

proposed by Lionberger and Russel.[32] This expression nearly conforms to the correct $O(\phi)$-limit (*i.e.*, $H_s^t = 1 - 1.83\phi + O(\phi^2)$) and predicts H_s^t to vanish at random close packing $\phi = 0.64$. As seen in Fig. 3, the deviations from short-time SE scaling are smaller than from SED scaling (*e.g.*, $H_s^t\eta_\infty/\eta_0 = 1.4$ at $\phi = 0.45$ whereas $H_s^r\eta_\infty/\eta_0 = 3.1$). As shown elsewhere,[18,21] deviations from long-time SE scaling ($H_L^t\eta_L/\eta_0 = 1$) are even smaller than the deviation for short times in Fig. 3.

We mention that for translational diffusion an alternative SE relation has been proposed,[18] which links the high-frequency-limiting viscosity to the short-time collective diffusion coefficient $D_s^c(q_m)$:

$$D_s^c(q_m) = \frac{k_B T}{6\pi\eta_\infty(\phi)a}. \tag{17}$$

The coefficient $D_s^c(q_m) = D_0^t H(q_m)/S(q_m)$, measured at the wave number q_m where the static structure factor attains its maximum $S(q_m)$, quantifies the short-time relaxation of the

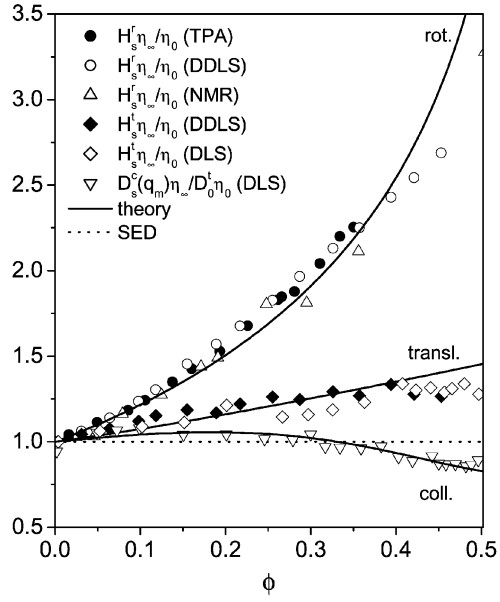

Fig. 3 Test of the validity of the rotational/translational short-time SE(D) scaling relations $H_s^a\eta_\infty/\eta_0 = 1$ (dotted line) with a = {r,t}, and η_∞/η_0 as in eqn. (12). The drawn lines are theoretical results for $H_s^a\eta_\infty/\eta_0$, with H_s^r according to eqn. (15) and H_s^t as in eqn. (16). Also shown are results for $H_s^r\eta_\infty/\eta_0$ with experimental data for H_s^r obtained with TPA,[14] DDLS,[11] and NMR,[37] and results for $H_s^t\eta_\infty/\eta_0$ with H_s^t measured using DDLS[11] and DLS.[38] For comparison, results for $D_s^c(q_m)\eta_\infty/D_0^t\eta_0$ *versus* ϕ are included, with $D_s^c(q_m)$ calculated as explained in the text (drawn line), and measured using DLS.[38]

next-neighbor cage around a tracer particle. Collective diffusion is influenced by HI *via* the hydrodynamic function $H(q_m)$ and by DI *via* the peak height of the static structure factor $S(q)$ at the wave number q_m. For hard spheres up to $\phi = 0.5$, it has been shown[18] that $H(q_m) = 1 - 1.35\phi$ and $S(q_m) = 1 + 0.664\phi g^{(2)}(2a^+)$, with the Carnahan–Starling contact value expression[39] $g^{(2)}(2a^+) = (1 - 0.5\phi)/(1 - \phi)^3$. As seen from Fig. 3, the collective short-time SE relation $D_s^c(q_m)\eta_\infty/D_0^t\eta_0 = 1$ with η_∞/η_0 according to eqn. (12), is obeyed much better than the translational SE relation for H_s^t. The collective SE relation holds quite accurately up to $\phi = 0.35$, as confirmed by DLS[38] (open triangles in Fig. 3). Interestingly enough, the corresponding long-time SE relation $D_L^c(q_m)\eta_L/D_0^t\eta_0 = 1$, where $D_L^c(q_m)$ with $D_L^c(q_m) < D_s^c(q_m)$ is the long-time collective diffusion coefficient at q_m, is also approximately fulfilled for hard spheres, as shown by Segrè *et al.*[21] (We note that $D_L^c(q_m)$ exists only for wavenumbers $q \approx q_m$ and for sufficiently large particle concentrations.[18])

In the case of molecular diffusion, deviations from SE(D) scaling are often rationalized by arguing that hydrodynamic coupling between tracer and solvent changes from stick to (perfect) slip boundary conditions when the tracer particle approaches the molecular dimensions of the solvent molecules. Empirically, perfect slip is found for translational tracer diffusion (*i.e.* $f_0^t = \nu_0^t 6\pi\eta_0 a_T$ with $\nu_0^t = 2/3$)[40,41] and mixed slip–stick conditions for rotational tracer diffusion ($f_0^r = \nu_0^r 8\pi\eta_0 a_T^3$ with $0 < \nu_0^r < 1$).[5–7,42–44] These findings prompted us to employ a similar empirical approach to rationalize deviations from rotational short-time SED scaling of colloidal hard spheres. For this purpose, we express the reduced viscosity η_∞/η_0 as a sum $\eta_\infty/\eta_0 = 1 + \Delta\eta_\infty$ of a solvent contribution and an excess part $\Delta\eta_\infty = 2.5\phi + O(\phi^2)$. Further, we replace the Stokesian friction factor $f_s^r = 8\pi\eta_\infty a_T^3$ in eqn. (3) by a sum over the rotational drag due to the solvent alone (which sticks) plus an additional drag due to the (hydrodynamic) interactions of the tracer sphere with the host particles. As argued for the translational case already by Imhof *et al.*,[45] there is no reason to expect a no-slip boundary condition for the host particle contribution. We thus modify f_s^r as

$$f_s^r(\phi) = 8\pi\eta_0 a_T^3[1 + \nu_s^r\Delta\eta_\infty(\phi)] \tag{18}$$

with an apparent slip coefficient $\nu_s^r \in [0,1]$ determined from demanding that $D_s^r(\phi,\lambda) = k_B T/f^t(\phi,\lambda)$. The coefficient $\nu_s^r = \nu_s^r(\phi,\lambda)$ depends in principle also on the nature of the DI between the spheres. However, for hard-sphere suspensions ν_s^r depends only on the tracer/host size ratio λ and, to some extent, also on ϕ. The stick value $\nu_s^r = 1$ is attained only in the continuum limit $\lambda \gg 1$, when the tracer is much larger than the host particles. Moving away from the continuum limit by lowering λ leads to values $\nu_s^r < 1$, reflecting the locally discontinuous nature of the neighborhood around a tracer sphere (which changes with ϕ). In the limit $\lambda \ll 1$ of a point-like tracer (relative to a host sphere) one expects nearly perfect slip $\nu_s^r \approx 0$.[46] For small host concentrations, *i.e.* to linear order in $\phi \ll 1$, $\nu_s^r(\lambda)$ is independent of ϕ. For hard spheres it follows then readily from eqns. (9) and (18) that

$$\nu_s^r(\lambda) = -\frac{2}{5} h_1^r(\lambda), \tag{19}$$

where $h_1^r(\lambda)$ is the first virial coefficient of $H_s^r(\phi,\lambda)$. As will be shown later in section V, $h_1^r = 0$ for $\lambda \to 0$ and $h_1^r = -2.5 + O(\lambda^{-1})$ for $\lambda \to \infty$, in accordance with the qualitative description of the λ-dependence of $\nu_s^r(\phi,\lambda)$ given above. We note that the λ-dependence of the apparent slip coefficient $\nu_s^r(\lambda)$ was investigated first by Almog and Brenner.[46] A similar analysis has been made for translational short-time diffusion.[16] Similar to eqn. (18), a modified Stokesian friction factor $f_s^t(\phi)$ can be written for translation, according to $f_s^t(\phi) = 6\pi\eta_0 a_T[1 + \nu_s^t \Delta\eta_\infty(\phi)]$.

The apparent slip parameters ν_s^a for rotation (a = r) and translation (a = t) can be deduced from experimental data by plotting

$$\nu_s^a = \frac{D_0^a/D_s^a - 1}{\eta_\infty/\eta_0 - 1}. \tag{20}$$

Fig. 4 shows such a plot using the experimental hard-sphere data for H_s^r and H_s^t with $\lambda = 1$ as included in Fig. 2, and taking eqn. (12) for η_∞/η_0. The drawn lines represent the theoretical predictions for ν_s^r and ν_s^t obtained from eqns. (15) and (16) respectively. As can be seen, the calculated ν_s^r and ν_s^t are only weakly dependent on ϕ, so that the average values $\nu_s^r = 0.22$ (partial slip) and $\nu_s^t = 0.67$ (close to perfect slip) are reasonable overall estimates for the full fluid concentration range $\phi < 0.5$. In fact, eqn. (18) for $f^t(\phi)$ with $\nu_s^r = 0.22$ leads to a remarkably good prediction for $H_s^r(\phi)$ (*cf.* the dotted line in Fig. 2).

An analogous analysis in terms of apparent slip parameters for $\lambda = 1$ was done by Lionberger and Russel[47] for short-time translational self-diffusion, and by Imhof *et al.*[45] and Segrè *et al.*[21] for long-time translational self-diffusion. At short times theory and experiment (*cf.* Fig. 4) suggest an

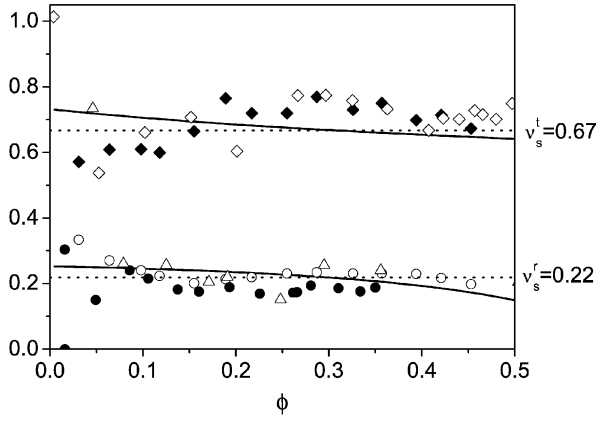

Fig. 4 Slip coefficients ν_s^r and ν_s^t from eqn. (20), for rotational and translational short-time tracer diffusion in host sphere dispersions, using experimental data for H_s^r (symbols are the same as in Fig. 3) and the theoretical expression eqn. (15) (drawn lines), with η_∞/η_0 obtained from eqn. (12). Dotted lines represent overall averages $\nu_s^r = 0.22$ and $\nu_s^t = 2/3$.

average translational slip parameter ν_s^t close to the value 2/3 of perfect slip. For long times, Segrè *et al.*[21] reported a monotonic decline of ν_L^t from 1 (no slip) at small ϕ to 0.67 (perfect slip) at $\phi = 0.5$. For charged particles, Imhof *et al.*[45] determined an average long-time slip parameter $\nu_L^t \approx 0.5$ which, for unknown reasons, is even smaller than the perfect slip value 2/3.

We emphasize that the concept of an apparent slip parameter merely provides a qualitative picture to rationalize deviations from ideal SED scaling. Actually, SE(D) scaling cannot even be exact for arbitrary ϕ, since the leading order low density forms $1 + A\phi + B\phi^2$ are different for diffusion and inverse viscosity ($A = -0.63$ for H_s^r and -1.83 for H_s^t, while $A = -2.5$ for η_0/η_∞).

IVb Long-time rotational tracer diffusion

The coefficient $D_L^r = H_L^r D_0^r$ is, contrary to the long-time translational self-diffusion coefficient $D_L^t = H_L^t D_0^t$, not a true long-time property. The coefficient D_L^t is well-defined as the long-time asymptotic slope of the particle mean-squared displacement.[29,48] The latter depends linearly on time both at short and long times (diffusive regimes) with a sublinear regime at intermediate times. Correspondingly, rotational Brownian motion is diffusive only if the (DDLS) single particle orientational correlation function $C_2(t)$ is single-exponentially decaying in time t. In general, this is only the case for a tracer sphere in pure solvent ($C_2(t) \propto \exp[-6D_0^r t]$) and for a tracer in a host suspension at short times ($C_2(t) \propto \exp[-6D_s^r t]$), as shown by Jones and Felderhof.[17,49,50] For dilute monodisperse hard-sphere suspensions, it has been shown theoretically[17] that $C_2(t)$ is non-exponential at intermediate and long times, *viz.*

$$\frac{C_2(t)}{C_2^{(0)}(t)} = 1 + \gamma_2(t)\phi + O(\phi^2), \tag{21}$$

where $\gamma_2(t)$ was computed numerically for hard spheres with two-body HI included. While a long-time rotational diffusion coefficient cannot be defined, one can always define instead a mean orientational diffusion coefficient, D_L^r, through[17,49,50]

$$\frac{1}{6D_L^r} = \tau_L^r = \int_0^\infty \mathrm{d}t C_2(t) = \frac{1}{6D_0^r}\left[1 - C_L^r\phi + O(\phi^2)\right], \tag{22}$$

with $C_L^r = 0.67$ for hard spheres. Memory effects in $C_2(t)$ lead thus to a mean diffusion coefficient D_L^r, only slightly smaller than D_s^r to first order in ϕ. At present, neither theoretical nor experimental results are available to verify to what extent D_L^r scales with the inverse low-shear viscosity η_0/η_L. To order ϕ, SED scaling is certainly not valid, since C_L^r is much smaller than the first virial coefficient of η_0/η_L, which equals -2.5. Similarly, SE scaling of long-time translational diffusion[51,52] is not exact to order ϕ, since $H_L^t = 1 - 2.10\phi$.

DDLS experiments on dense hard-sphere-like PFA suspensions[11] support the non-diffusive rotational long-time regime predicted by theory[17] and quantitatively agree with the theoretical prediction for $\gamma_2(t)$ for $\phi < 0.2$ and times $t < 1/(2D_0^r)$. For $\phi > 0.2$, $\gamma_2(t)$ determined from DDLS is larger than predicted by theory. Contrary to the DDLS experiments, in our TPA experiments we find no significant deviation from a single-exponential decay of $C_2(t)$ even at high volume fractions and times up to $t \approx 4/(3D_0^r)$. We mention in this context that $C_2(t)$ is measured directly with TPA,[30,53] whereas $C_2(t)$ is determined only indirectly using DDLS.[11] The latter method invokes a translation–rotation decoupling approximation to extract $C_2(t)$ from the DDLS autocorrelation function $g_{VH}(t)$. This approximation becomes exact only in the limit of small concentrations and short times.[11]

V SED scaling in binary hard-sphere mixtures

In the following we explore rotational self-diffusion of an infinitely dilute neutral tracer component in a hard-sphere host suspension for $\lambda \neq 1$, and its relation to the shear viscosity. For comparison, we also report on results for SE scaling of translational tracer diffusion.

Fig. 5 shows approximate theoretical results, according to eqn. (9), for the short-time rotational and translational first virial coefficients, $h_1^r(\lambda)$ and $h_1^t(\lambda)$ respectively, of $H_s^r(\phi,\lambda)$ and $H_s^t(\phi,\lambda)$. Both

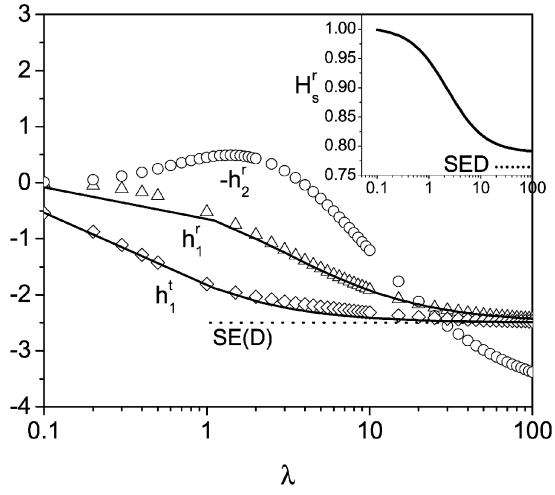

Fig. 5 Calculated rotational/translational first virial coefficients $h_1^r(\lambda)$ and $h_1^t(\lambda)$, and rotational second virial coefficient $h_2^r(\lambda)$. The single-parameter forms $h_1^{(a)} = -2.5[1 + c_a\lambda^{-1}]^{-1}$ with $c_r = 3.0$ and $c_t = 0.366$ respectively are shown for comparison (drawn lines). The dotted line is the SE(D) continuum limit $h_1^r = h_1^t = -2.5$. The inset shows the λ-dependence of $H_s^r(\lambda,\phi)$ for $\phi = 0.1$; the dotted line in the inset is the SED continuum prediction $H_s^r = 0.76$.

virial coefficients decrease monotonically from 0 at $\lambda = 0$ to the Einstein value -2.5 in the continuum limit $\lambda \to \infty$. In accordance with our discussion of the generic λ-dependence of ν_s^r and ν_s^t in section IV, a point-like tracer with $\lambda = 0$ experiences only solvent friction, whereas at very large λ the host dispersion acts as a continuous fluid of effective viscosity $\eta_\infty = \eta_0[1 + 2.5\phi]$. The theoretical results for h_1^a are rather well parametrized by the form[16]

$$h_1^a(\lambda) = \frac{-2.5}{1 + c_a\lambda^{-1}}, \tag{23}$$

with $c_a = 3.0$ for a = r and 0.366 for a = t, so that $h_1^a(\lambda) = -2.5 + O(\lambda^{-1})$ for $\lambda \to \infty$. Eqn. (23) agrees within 5% with calculations of $h_1^r(\lambda)$ by Batchelor,[51,54] who included numerical lubrication corrections. Likewise, eqn. (23) is in good qualitative agreement with low-density calculations of $\nu_s^r(\lambda)$ by Almog and Brenner.[46] Fig. 5 demonstrates that $h_1^r(\lambda)$ decays somewhat faster towards the asymptotic SE(D) value -2.5 than $h_1^r(\lambda)$. This is due to the weaker asymptotic r^{-4} long-distance decay of the translational mobility function as compared to the r^{-6} decay of the rotational mobility function.

Numerical results for the rotational second virial coefficient $h_2^r(\lambda)$ are also included in Fig 5. Corresponding results for $h_2^t(\lambda)$ are discussed in ref. 16. It can be seen that $h_2^r(\lambda)$ is non-monotonic with a minimum value at $\lambda \approx 1.2$. It changes sign from negative to positive values at $\lambda = 3.8$. The inset shows $H_s^r(\phi,\lambda)$ according to eqn. (9), for a fixed $\phi = 0.1$. Rotational tracer diffusion is strongly slowed down with increasing tracer/host size ratio λ, but the SED limit $H_s^r = [\eta_0/\eta_\infty(\phi = 0.1)] = 0.76$ is approached only at very large values of λ. It should be noted, however, that the truncated virial expansion in eqn. (9), with far-field $O(r^{-12})$ pair and $O(r^{-9})$ triplet HI included, most likely overestimates $H_s^r(\phi,\lambda)$ for large λ. For large λ, a tracer interacts with more than two host spheres at a time, unless ϕ is very small, leading to an enhanced hydrodynamic hindrance of rotational motion. A further reduction in H_s^r may arise from near-field lubrication effects, which are not included in our calculations. Thus, we expect that the actual $H_s^r(\phi,\lambda)$ will approach the SED continuum limit for smaller λ than suggested by eqn. (9).

Our rotational diffusion measurements by TPA for $\lambda \leqslant 1$ and by DDLS for $\lambda > 1$ confirm that $H_s^r(\phi,\lambda)$ decreases strongly with increasing λ (see Fig. 6A). However, theory and experiment are not in quantitative agreement for the asymmetric cases $\lambda = 0.33$ and $\lambda = 10$. This is partially due to a

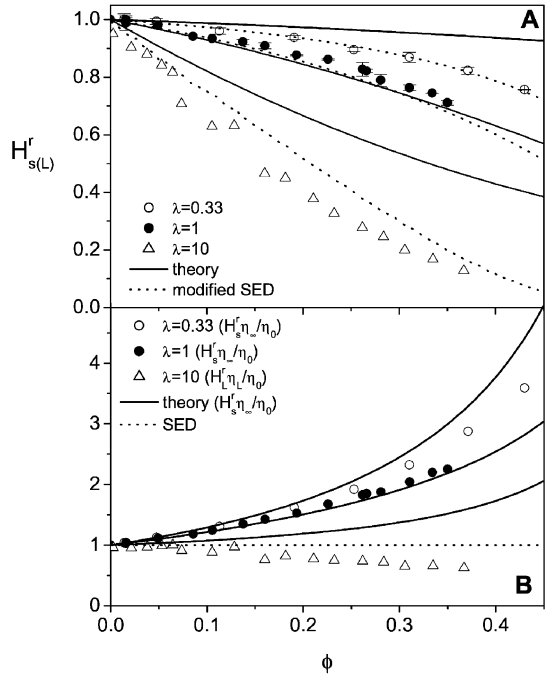

Fig. 6 A: Reduced short-time (long-time) rotational diffusion coefficient for tracer/host size ratios $\lambda = 0.33$ and 1 (TPA:H_s^r) and $\lambda = 10$ (DDLS:H_L^r). Drawn lines represent the theoretical short-time predictions in eqn. (9). Dotted lines are the modified SED results of eqn. (18) with $\nu_s^r = 0.089$ ($\lambda = 0.33$), $\nu_s^r = 0.22$ ($\lambda = 1$), and $\nu_s^r = 1$ ($\lambda = 10$). B: Test of SED scaling relations (dotted line) $H_s^r\eta_\infty/\eta_0 = 1$ (for $\lambda = 0.33$ and 1) and $H_L^r\eta_L/\eta_0 = 1$ (for $\lambda = 10$) with η_∞/η_0 as in eqn. (12), and η_0/η_L taken from ref. 18, H_s^r and H_L^r measured with TPA and DDLS respectively, and theoretical predictions for $H_s^r\eta_\infty/\eta_0$ ($\lambda = 0.33$–10) obtained with eqns. (9) and (12) (drawn lines).

shrinkage of the ϕ-interval where our approximate theoretical treatment applies with increasing size asymmetry. For large λ there is an additional reason for the observed difference in H_s^r between experiment and theory: DDLS experiments then actually determine the long-time rotational motion of a tracer, since the host particles diffuse much faster than the tracer. While in principle a long-time rotational diffusion coefficient D_L^r does not exist for $\lambda = 1$, we nevertheless expect that a true long-time diffusive regime characterized by a well-defined D_L^r is recovered in the limit of large λ. There is indeed no indication in our DDLS measurements at $\lambda = 10$ for any non-exponential long-time decay of $C_2(t)$. The memory effects associated with the time evolution of the host particle configuration thus lead to an additional reduction in the measured diffusion coefficient D_L^r.[17,49,50]

Fig. 6B provides a test of the accuracy of SED scaling for binary hard-sphere suspensions for various λ. The TPA data for $\lambda \leqslant 1$ are multiplied by eqn. (12) for $\eta_\infty(\phi)/\eta_0$, whereas the DDLS data for $\lambda \leqslant 10$ are multiplied by the (''long-time'') zero-shear-limiting viscosity $\eta_L/(\phi)/\eta_0$ of hard spheres calculated using mode-coupling-theory.[55] For comparison, Fig. 6B displays also our truncated cluster expansion results for H_s^r according to eqn. (9), multiplied by $\eta_\infty(\phi)/\eta_0$. With increasing λ, both the theoretical and experimental data approach the SED relation $H_s^r\eta_\infty(\phi)/\eta_0 = 1$. The experimental values of $H_L^r\eta_L(\phi)/\eta_0$ for $\lambda = 10$ are slightly smaller than one, probably due to the presence of depletion attractions between the tracers induced by the smaller host spheres. The tracer concentration in the experiments is thus not infinitely small, as it is assumed in the theoretical calculations. The attractions, however, do not affect long-time translational diffusion (*i.e.* $H_L^t\eta_L/\eta_0 \approx 1$ for all ϕ).[25]

As already discussed, an intuitive way to interpret deviations from SED scaling at different λ is to introduce the apparent slip coefficient $\nu_s^r(\phi,\lambda)$ in eqn. (18) which varies continuously between 0 for

$\lambda \to 0$ (perfect slip) and 1 for $\lambda \to \infty$ (perfect stick). The experimental data for $\lambda = 0.33$ are overall well described by the modified SED relation in eqn. (18) using a value $\nu_s^r = 0.089$ (see dotted line in Fig. 6A). For values of λ between 0.24 and 1 we find a monotonic increase of ν_s^r from 0.071 to 0.22 (*cf.* Table 1). Using short-time calculations to first order in ϕ according to eqn. (19), somewhat smaller values for ν_s^r are found (Table 1), due to an overestimation of H_s^r at larger ϕ. Experiments are currently underway to characterize the λ-dependence of H_s^r and ν_s^r more completely in the range $\lambda \in [0.1–20]$, using DDLS applied to PFA tracers in host suspensions of refractive index matched fluorinated latex spheres.[56]

VI SED scaling for suspensions of charged spheres

VIa Short-time rotational tracer diffusion

Our theoretical calculations of the short-time diffusion of a charged tracer sphere in a host suspension of charged spheres predict that $H_s^r(\phi,\lambda)$ (and $H_s^t(\phi,\lambda)$) increases with decreasing ionic strength of the supporting electrolyte, since the hydrodynamic coupling between strongly repelling charged spheres is weaker than between neutral ones. This can be seen from the integrals in eqns. (7) and (8) for H_{s1}^r and H_{s2}^r. Both quantities are equilibrium averages of hydrodynamic self-mobility functions. Since the self-mobility functions are rather short-ranged (the leading asymptotic term is proportional to r^{-6} for rotation and proportional to r^{-4} for translation), the main contribution to the integrals stems from configurations with two or more particles close to contact. For neutral spheres, $g_{TH}^{(2)}$ and $g_{HH}^{(2)}$ attain their maximum at contact. For charged spheres these maxima are shifted to larger distances, which results in reduced hydrodynamic coupling.

Experimental TPA data for $\lambda \leqslant 1$ at various concentrations of added LiCl (0, 10 and 100 mM) confirm this theoretical prediction (Fig. 7). We note that the suspensions with 0 mM added LiCl still contain about 0.1 mM residual univalent electrolyte. A close comparison between the TPA

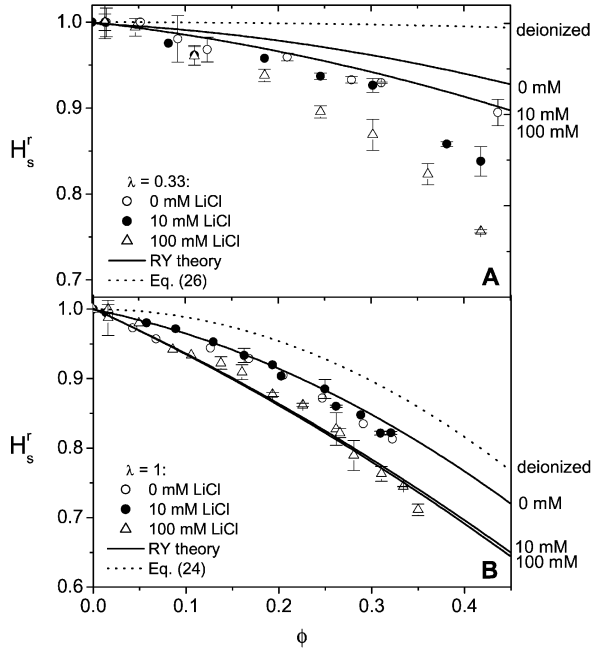

Fig. 7 Reduced short-time rotational diffusion coefficient H_s^r of charged spheres obtained with TPA for *added* concentrations of LiCl of 0, 10 and 100 mM, in comparison with RY-based calculations (drawn lines). A: size ratio $\lambda = 0.33$; $Z_T = 220$, $Z_H = 1200$, and 0.2 mM residual 1–1 electrolyte. B: size ratio $\lambda = 1$; $Z_T = Z_H = 220$, $a_T = 90$ nm, and 0.1 mM residual 1–1 electrolyte. The dotted lines represent the theoretical prediction for fully deionized suspensions of charged spheres according to eqn. (26), with $a_r = 1.28$.

data and our RY-based calculations (drawn lines) reveals some differences. For all systems considered with $\lambda < 1$ (*i.e.* $\lambda = 0.24$, 0.33 (Fig. 7A), 0.34 and 0.46) we find $H_s^r(0\ \text{mM}) > H_s^r(10\ \text{mM}) > H_s^r(100\ \text{mM})$ for the experimental data, whereas theory predicts that $H_s^r(0\ \text{mM}) > H_s^r(10\ \text{mM}) \approx H_s^r(100\ \text{mM})$, since the $g_{TH}^{(2)}$ and $g_{HH}^{(2)}$ calculated within the RY scheme are nearly identical for 10 mM ($\kappa a = 0.026$) and 100 mM ($\kappa a = 0.008$). Furthermore, the theoretical results are systematically larger than the experimental data (see Fig. 7A). For $\lambda = 1$ (Fig. 7B) we find from TPA that $H_s^r(0\ \text{mM}) \approx H_s^r(10\ \text{mM}) > H_s^r(100\ \text{mM})$, which is again different from the theoretical prediction. These discrepancies may be due to details in the experimental interaction potential (*e.g.* solvation effects) which are not addressed in our calculations. Moreover, the calculations are based on the simplifying assumptions that the effective charges Z_T and Z_H are independent of ionic strength and ϕ.

In order to test the validity of SED scaling, the short-time diffusion data should be compared to corresponding high-frequency-limiting viscosity data for the same host suspensions. Unfortunately, neither experimental data nor complete theoretical predictions of η_∞ as a function of κ^{-1} and ϕ are currently available, so that this comparison is left to future investigations.

However, in the limit of zero added salt there exists a theoretical prediction of η_∞ (eqns. (13) and (14)). Also, calculations of H_s^r and H_s^t have been performed in this limit. For monodisperse suspensions of strongly charged spheres, theory predicts nonlinear volume fraction dependences,[12,14,15,57]

$$H_s^r(\phi) = 1 - a_r\phi^2, \tag{24}$$

and

$$H_s^t(\phi) = 1 - a_t\phi^{4/3}, \tag{25}$$

with parameters $a_r \approx 1.3$ and $a_t \approx 2.5$ which depend only weakly on the particle charge. The occurrence of the non-linear exponents 2 and 4/3 can be understood in terms of an effective hard-sphere model,[12] with a ϕ-dependent effective particle diameter which scales as $\phi^{-1/3}$. Eqns. (24) and (25) have recently been confirmed by lattice Boltzmann simulations,[36] DDLS,[58] and DLS.[59] It was shown that eqn. (24) applies up to $\phi \approx 0.3$, whereas eqn. (25) is applicable only for $\phi < 0.1$.[12] The generalization of eqn. (24) to rotational tracer diffusion with $\lambda \neq 1$ reads:[15]

$$H_s^r(\phi,\lambda) = 1 - a_r\lambda^3\phi^2, \tag{26}$$

with an applicable ϕ-range which shrinks with increasing size and interaction asymmetry. Note that the experimental TPA data for silica spheres in DMSO–DMF with zero added LiCl (Fig. 7) are located below the predictions in eqns. (24) and (26) for fully deionized suspensions (dotted lines), indicating that these suspensions contain a significant residual salt concentration (~0.1 mM univalent salt[25]).

Fig. 8 summarizes, for $\lambda = 1$, the typical scaling behaviour of the short-time rotational, translational, and collective reduced diffusion coefficients H_s^r (eqn. (24)), H_s^t (eqn. (25)) and $D_s^c(q_m)/D_0^t$, all multiplied by the reduced viscosity $\eta_\infty(\phi)/\eta_0$ of deionized charge-stabilized suspensions as quoted in eqn. (14). The depicted ϕ-range is much smaller than the one for hard spheres in Fig. 3, since for $\phi = 0.1$ the charged particles are already strongly correlated. To calculate the collective diffusion coefficient $D_s^c(q_m)$ we use the parametric form $H(q_m) = 1 + p_c\phi^{0.4}$ with $p_c = 1.5$, and $S(q_m)$ is calculated using for simplicity the rescaled mean spherical approximation.[18] While H_s^r and H_s^t are nearly charge-independent, as long as the physical hard-core remains completely masked, $D_s^c(q_m)$ decreases with increasing charge for given ϕ, mainly due to the strong charge-dependence of the structure factor peak height $S(q_m)$.[18] Fig. 8 illustrates that the deviations from SE(D) scaling $H_s^{(a)}\eta_\infty(\phi)/\eta_0 = 1$ for rotation (a = r) and translation (a = t) are similar in magnitude as for hard spheres. In contrast, deviations from the collective SE relation $D_s^c(q_m)\eta_\infty/D_0^t\eta_0 = 1$ are significantly larger than for hard spheres. There is a steep decrease of $D_s^c(q_m)\eta_\infty/D_0^t\eta_0$ from 1 at $\phi = 0$ towards a minimal value of 0.4 at $\phi \approx 0.005$ followed by a slight increase at larger ϕ. Fig. 8 indicates that short-time SE(D) scaling fails for deionized dispersions with $\lambda = 1$. Mode-coupling theory calculations[18] suggest a failure also for long-time translational self- and collective diffusion.

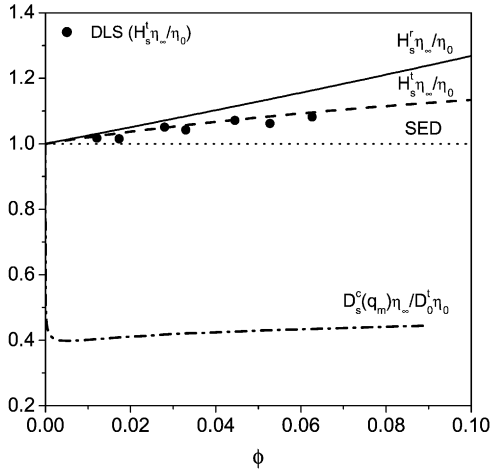

Fig. 8 Theoretical test of SE(D) scaling relations $H_s^a\eta_\infty/\eta_0 = 1$ (dotted line) with a = {r,t}, and $D_s^c(q_m)\eta_\infty/D_0^t\eta_0 = 1$, for typical deionized charge-stabilized suspensions, with η_∞/η_0 as in eqn. (14), and H_s^a calculated using eqns. (23) and (24). The calculation of $D_s^c(q_m)$ is explained in the text. For comparison, we further show DLS results[59] for H_s^t, multiplied by η_∞/η_0 calculated from eqn. (14).

To our knowledge, so far no calculations exist of long-time rotational motion in charged-sphere suspensions.

VIb Long-time rotational tracer diffusion

Using DDLS, we have measured the dependence of $H_L^r(\phi)$ on the concentration of added salt (*i.e.* NaCl) for the strongly asymmetric case of $\lambda = 10$. Fig. 9A shows a non-monotonic dependence of H_L^r on the concentration of added NaCl and, for zero added salt, also a non-monotonic dependence of H_L^r on the host volume fraction for small ϕ. Increasing the amount of NaCl from 0 to 1 mM reduces H_L^r, while enlarging the NaCl content from 1 to 10 mM gives rise instead to a small enhancement. This peculiar non-monotonic behavior of H_L^r must be due to a delicate competition of short-time effects and memory contributions arising from HI and DI. Computer simulations and theory are needed to analyze this interesting interplay of HI and DI.

The product of the experimental H_L^r with the experimentally determined zero-shear-limiting reduced viscosity $\eta_L(\phi)/\eta_0$ is plotted *versus* ϕ (for each salt content) in Fig. 9B. For zero added salt, long-time tracer diffusion is substantially faster than predicted on the basis of the long-time SED relation. However, on addition of salt, SED scaling $H_L^r\eta_L/\eta_0 = 1$ is approached. We remark that for given $\phi > 0.25$, $\eta_L(\phi)/\eta_0$ increases quite strongly with decreasing amount of added salt (*cf.* inset of Fig. 9A).

Qualitatively, it is understandable that SED scaling fails at low ionic strength. In dispersions with no added salt the dynamics of the host particles is strongly coupled to the tracer by long-range electrical double layer interactions. Hence, the tracer does not experience an effective fluid (*i.e.* $H_L^r\eta_L/\eta_0 > 1$) since the effective structural relaxation time of the host particles is no longer small compared to the reorientation time of a tracer sphere. With increased screening of electrostatic interactions the structural relaxation time of the host particles is reduced, and the host suspension appears to the tracer more and more as a continuous medium.

VII SED scaling for tracer sphere diffusion in isotropic rod suspensions

In sections IV to VI dealing with tracer sphere diffusion in suspensions of host spheres it has been shown that SED scaling (assuming stick boundary conditions) is less accurate in the case of slow host dynamics as compared to the tracer diffusion time scale, *i.e.* for small size ratios λ and strong

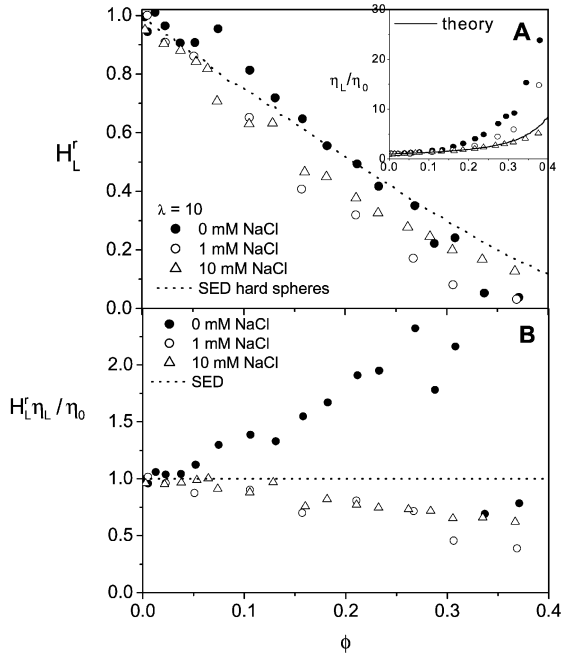

Fig. 9 A: DDLS results for the reduced long-time rotational diffusion coefficient H_L^r of charged spheres with $\lambda = 10$, in comparison with the SED scaling prediction $H_L^r = \eta_0/\eta_L$ for hard spheres with η_0/η_L from ref. 18 (dotted line). Inset shows measured reduced viscosity η_L/η_0 compared with the calculated viscosity.[18] B: Test of SED scaling of H_L^r, measured using DDLS, using the measured reduced inverse viscosity η_0/η_L.

double layer repulsions. An alternative way to manipulate the time scales of the orientational and translational motion of the host particles is to use anisotropic rod-like host particles instead of spheres. In particular rotational motion of rods is strongly hindered already at volume fractions much smaller than it is the case for spheres due to the stronger excluded volume structural correlations of rods.[60]

Here we present TPA results for the rotational diffusion of charged tracer spheres with three different radii, $a_T = 72$, 100 and 137 nm, in host suspensions of charged rods of aspect ratio $L/D = 203$ nm/18 nm = 11 in DMF. For all three types of tracers the ionic strength dependence of H_s^r (*cf.* Fig. 10A) is qualitatively similar to that measured for monodisperse host sphere suspensions in DMSO–DMF (Fig. 7B), *i.e.* $H_s^r(0\text{ mM}) \approx H_s^r(10\text{ mM}) > H_s^r(100\text{ mM})$. This result is quite remarkable in view of the experimental data on the low-shear viscosity, $\eta_L(\phi)$, of the rod suspensions as a function of LiCl concentration (Fig. 10C). Adding 1 mM LiCl to an initially salt-free dispersion of rods leads to a significant reduction of $\eta_L(\phi)$. Adding 10 mM LiCl leads to a further reduction. The viscosities for LiCl concentrations of 10 and 100 mM are practically equal and, for volume fractions below the rod overlap value ($\phi^* \approx 0.008$), close to the theoretical prediction of order ϕ^2 for hard rods.[61,62] Thus, rheology suggests hard-rod-like behavior for LiCl concentrations $\geqslant 10$ mM. In contrast, the rotational diffusion results show no evidence of enhanced screening of electrostatic repulsions at 10 mM LiCl as compared to 0 mM LiCl. Further, the TPA experiments suggest that the interaction potential with 10 mM added LiCl is not the same as with 100 mM. Perhaps this is related to particle solvation by DMF, causing a strong repulsion at short interparticle distances ($\sim$3 nm) which is noticeable only at high salt contents.[26] A comparison with the experimental results for binary sphere dispersions shows that rotational diffusion is much more effectively hindered by rods than by spheres. Qualitatively this can be explained by the stronger excluded volume correlations between rods as compared to spheres.

For testing SED scaling in rod–sphere mixtures, one needs experimental data and/or a theoretical expression for the infinite-frequency viscosity $\eta_\infty(\phi)$ of suspensions of (charged) rods.

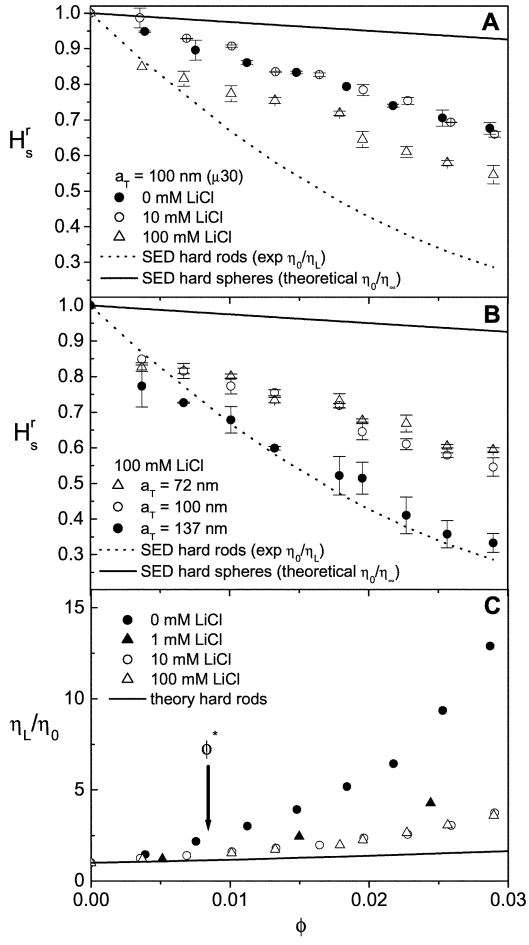

Fig. 10 Rotational diffusion coefficient H_s^r of charged tracer spheres dispersed in host suspensions of charged rods. A: Effect of LiCl concentration for the tracer sphere μ30 (with $a_T = 100$ nm, *cf.* Table 1). B: Dependence of H_s^r on tracer radius a_T for a LiCl concentration of 100 mM. The dotted lines in Fig. 10A and B represent SED scaling based on the experimental η_L, assuming complete stick; drawn lines are SED scaling results based on eqn. (12) for the η_∞ of hard spheres with complete stick. C: Measured reduced low-shear-limiting viscosity η_L/η_0 of host-rod suspensions for various LiCl concentrations as indicated. The rod overlap volume fraction is $\phi^* = 0.008$.

Since these are not available at present, we compare H_s^r with the reciprocal of the experimentally determined hard-rod low-shear viscosity $\eta_L(\phi)$. Fig. 10A reveals that rotational diffusion of 100 nm tracers is, for all ϕ and salt concentrations considered, faster than expected on the basis of the inverse hard-rod viscosity η_0/η_L. Deviations from η_0/η_L become smaller with increasing ionic strength (for instance at $\phi = 0.03$, $H_s^r\eta_L/\eta_0 = 8$ for 0 mM added LiCl and $H_s^r\eta_L/\eta_0 = 2$ for 100 mM added LiCl). The graph of the inverse high-frequency viscosity η_0/η_∞ of charged rods is most likely located in between the dotted line in Fig. 10A (η_0/η_L for rods) and the drawn line (η_0/η_∞ for spheres). Thus, we expect that $H_s^r\eta_\infty/\eta_0 < 2$ for 100 mM LiCl.

For given ionic strength, deviations from SED scaling with η_0/η_L become smaller with increasing tracer size. This is illustrated in Fig. 10B for $c_{LiCl} = 100$ mM. For the largest tracer, coded as "P113" (with $a_T = 137$ nm and $\sigma = 10\%$), $H_s^r\eta_L/\eta_0 = 1$. This trend is analogous to that observed for binary hard-sphere suspensions (Fig. 6).

VIII Summary and conclusions

With respect to short-time rotational diffusion of tracers in suspensions of uncharged host spheres clear conclusions can be drawn from both the theoretical and the experimental results. SED scaling of the rotational tracer diffusion coefficient with the inverse macroscopic host viscosity fails, unless the interaction time scale of the tracer sphere is much larger than that of the host spheres, as is the case for tracer/host size ratios $\lambda \gg 1$. Then the host spheres respond instantly, so the tracer experiences the host suspension as a continuous solvent with an effective viscosity close to the macroscopic value. When the host particle interaction time scale is comparable to that of the tracer ($\lambda \approx 1$), the tracer experiences a discontinuous host fluid, producing a viscous drag which shifts towards the drag that would be caused by the pure solvent, so $H_s^r \eta_\infty(\phi)/\eta_0 > 1$. In the extreme case $\lambda \ll 1$, the point-like tracer rotates in an essentially static environment of host spheres and the tracer dynamics is affected (for times $t \ll \tau_0^1$) only by the solvent viscosity η_0. The effect of a discontinuous host fluid on tracer rotation can be modelled by an apparent slip coefficient in the Stokesian friction factor that varies continuously in λ from complete stick for $\lambda \gg 1$ to complete slip for $\lambda \ll 1$. Applying the SED relation in a modified form by assuming partial slip (with $0 < \nu_0^r < 1$) leads to a reasonable heuristic description of the ϕ-dependence of rotational tracer diffusion.

With respect to the long-time rotational motion of tracers in suspensions of uncharged host spheres the situation is less clear. Theory and experiment show that D_L^r for $\lambda = 1$ is defined only as a mean diffusion coefficient describing the overall non-exponential decay of $C_2(t)$. On physical grounds (*i.e.* separation of time scales between tracer and host) we expect D_L^r to be a well-defined long-time property when $\lambda \gg 1$. Our DDLS experiments indicate that a size ratio $\lambda = 10$ is large enough to ensure that D_L^r is well-defined. Future (theoretical) work should explore the gradual changes in $C_2(t)$ from a non-exponential long-time behavior for $\lambda \geqslant 1$ to a diffusive exponential decay at large λ. An essentially unexplored field is the intermediate time regime of rotational motion, corresponding to finite frequencies. An interesting heuristic generalization of the SE relation for translational diffusion to finite strain frequencies ω was proposed by Mason and Weitz.[63] This relation is extensively used in microrheological experiments, to relate mean-square displacement measurements of tracer particles in colloidal suspensions and gels to the linear viscoelastic properties of the medium.[8,9] The applicability of the frequency-dependent SE relation of Mason and Weitz to monodisperse suspensions of charged and neutral spheres has been tested using mode-coupling theory.[18] The SE relation was found to be approximately valid for hard spheres, but it does not apply to charged spheres. However, its applicability to tracer diffusion in charge-stabilized suspensions should improve with increasing tracer size, when the host suspension acts more and more like a continuous viscoelastic medium.[64] In view of the partial success of the Mason and Weitz relation, it is thus of interest to explore also possible relationships between $C_2(t)$ and the frequency-dependent viscosity $\eta(\omega)$.

The conclusions so far relate to uncharged hard spheres. With respect to charged spheres we can conclude from our calculations, that at very low ionic strength large deviations from SED scaling may be expected at short times. Measurements of long-time rotational diffusion for $\lambda = 10$ show likewise large deviations from SED scaling for charged spheres, which decrease with increasing ionic strength. More experimental and theoretical work in the low-salt regime is required to quantify and substantiate these findings.

Regarding the shape of the host particles, a first set of experimental results on short-time rotational diffusion of tracer spheres in host suspensions of rods presented in this paper indicates a qualitatively similar behavior as observed for host suspensions of spheres. The major difference between host suspensions of rods and spheres is that for given volume fraction, the hydrodynamic hindrance of a tracer sphere is much stronger for rods than for spheres due to large excluded volume correlations between rods. To arrive at more quantitative conclusions, theoretical work is needed on tracer diffusion in rod suspensions and on the high-frequency-limiting viscosity of (charged) rods.

All work in this paper relates to SED scaling of the rotational diffusion of single tracers in colloidal host suspensions. An interesting follow-up would be to investigate the applicability of SED relations to collective particle reorientation, as appearing in the polarization fluctuations of colloidal spheres with electric or magnetic dipole interactions.[49,50] As mentioned in sections IV and

VI, SE relations for the translational collective diffusion coefficients $D_s^c(q_m)$ and $D_L^c(q_m)$ have already been tested both theoretically and experimentally. Interestingly, SE scaling was found to be valid to a good approximation for monodisperse hard spheres. However, it was shown to fail for charged spheres. To our knowledge, so far no attempts have been made to perform analogous tests of SED scaling for collective rotational diffusion.

Acknowledgements

We thank S. Sacanna, M. Pazzini, C. van Kats and D. van den Heuvel for preparing silica tracers, Ausimont for its kind gift of the PFA tracers, and J. K. G. Dhont, A. J. Banchio, M. Watzlawek, H. Ma, and W. K. Kegel for helpful discussions. This work was financially supported by The Netherlands Organization for Scientific Research (CW/NWO) and the National Natural Science Foundation of China.

References

1 G. Stokes, *Trans. Cambridge Philos. Soc.*, 1856, **9**, 5.
2 A. Einstein, *Ann. Physik (Leipzig).*, 1906, **19**, 371.
3 P. Debye, *Polar molecules*, Dover, New York, 1929.
4 B. J. Alder, D. M. Gass and T. E. Wainwright, *J. Chem. Phys.*, 1970, **53**, 3813.
5 C. M. Hu and R. Zwanzig, *J. Chem. Phys.*, 1974, **60**, 4354.
6 R. Zwanzig, *J. Chem. Phys.*, 1978, **68**, 4325.
7 M. Vergeles, P. Keblinski, J. Koplik and J. R. Banavar, *Phys. Rev. Lett.*, 1995, **75**, 232.
8 T. Gisler and D. A. Weitz, *Curr. Opin. Colloid Interface Sci.*, 1998, **3**, 586.
9 F. C. MacKintosh and C. F. Schmidt, *Curr. Opin. Colloid Interface Sci.*, 1999, **4**, 300.
10 R. B. Jones, *Physica A.*, 1988, **150**, 339.
11 V. Degiorgio, R. Piazza and R. B. Jones, *Phys. Rev. E.*, 1995, **52**, 2707.
12 M. Watzlawek and G. Nägele, *Physica A*, 1997, **235**, 56.
13 B. Cichocki, M. L. Ekiel-Jezewska and E. Wajnryb, *J. Chem. Phys.*, 1999, **111**, 3265.
14 G. H. Koenderink, H. Zhang, M. P. Lettinga, G. Nägele and A. P. Philipse, *Phys. Rev. E.*, 2001, **64**, 022 401.
15 H. Zhang and G. Nägele, to be submitted.
16 H. Zhang and G. Nägele, *J. Chem. Phys.*, 2002, **117**, 5908.
17 R. B. Jones, *Physica A*, 1989, **157**, 752.
18 A. J. Banchio, G. Nägele and J. Bergenholtz, *J. Chem. Phys.*, 1999, **111**, 8721.
19 M. M. Kops-Werkhoven and H. M. Fijnaut, *J. Chem. Phys.*, 1982, **77**, 2242.
20 A. van Blaaderen, J. Peetermans, G. Maret and J. K. G. Dhont, *J. Chem. Phys.*, 1992, **96**, 4591.
21 P. N. Segrè, S. P. Meeker, P. N. Pusey and W. C. K. Poon, *Phys. Rev. Lett.*, 1995, **75**, 958.
22 J. Bergenholtz, F. M. Horn, W. Richtering, N. Willenbacher and N. J. Wagner, *Phys. Rev. E.*, 1998, **58**, R4088.
23 C. W. J. Beenakker, *Physica A*, 1984, **128**, 48.
24 J. Kanetakis and H. Sillescu, *Chem. Phys. Lett.*, 1996, **252**, 127.
25 G. H. Koenderink and A. P. Philipse, *Langmuir*, 2000, **16**, 5631.
26 G. H. Koenderink, M. P. Lettinga and A. P. Philipse, *J. Chem. Phys.*, in press.
27 P. Mazur and W. van Saarloos, *Physica A*, 1982, **115**, 21.
28 D. J. Jeffrey and Y. Onishi, *J. Fluid Mech.*, 1984, **139**, 261.
29 G. Nägele, *Phys. Rep.*, 1996, **272**, 215.
30 M. P. Lettinga, C. M. van Kats and A. P. Philipse, *Langmuir*, 2000, **16**, 6166.
31 M. P. B. van Bruggen, *Langmuir*, 1998, **14**, 2245.
32 R. A. Lionberger and W. B. Russel, *J. Rheol.*, 1994, **38**, 1885.
33 J. Bergenholtz, N. Willenbacher, N. J. Wagner, B. Morrison, D. van den Ende and J. Mellema, *J. Colloid Interface Sci.*, 1998, **202**, 430.
34 F. M. Horn, W. Richtering, J. Bergenholtz, N. Willenbacher and N. J. Wagner, *J. Colloid Interface Sci.*, 2000, **225**, 166.
35 R. J. Philips, J. F. Brady and G. Bossis, *Phys. Fluids*, 1988, **31**, 3462.
36 M. H. J. Hagen, D. Frenkel and C. P. Lowe, *Physica A*, 1999, **272**, 376.
37 J. Kanetakis, A. Tolle and H. Sillescu, *Phys. Rev. E*, 1997, **55**, 3006.
38 P. N. Segrè, O. P. Behrend and P. N. Pusey, *Phys. Rev. E*, 1995, **52**, 5070.
39 J. P. Hansen and I. R. McDonald, *Theory of simple liquids*, Academic Press, London, 1986.
40 J. T. Hynes, *Ann. Rev. Phys. Chem.*, 1977, **28**, 301.
41 F. Ould-Kaddour and D. Levesque, *Phys. Rev. E*, 2000, **63**, 01 1205.
42 D. S. Alavi and D. H. Waldeck, *J. Phys. Chem.*, 1991, **95**, 4848.

43 R. S. Moog, D. L. Bankert and M. Maroncelli, *J. Phys. Chem.*, 1993, **97**, 1496.
44 G. B. Dutt and G. R. Krishna, *J. Chem. Phys.*, 2000, **112**, 4676.
45 A. Imhof, A. van Blaaderen, G. Maret and J. G. K. Dhont, *J. Chem. Phys.*, 1994, **100**, 2170.
46 Y. Almog and H. Brenner, *Phys. Fluids*, 1998, **10**, 750.
47 R. A. Lionberger and W. B. Russel, *Adv. Chem. Phys.*, 2000, **111**, 399.
48 J. K. G. Dhont, *An introduction to dynamics of colloids*, Elsevier, Amsterdam, 1996.
49 B. U. Felderhof and R. B. Jones, *Phys. Rev. E*, 1993, **48**, 1084.
50 B. U. Felderhof and R. B. Jones, *Phys. Rev. E*, 1993, **48**, 1142.
51 G. K. Batchelor, *J. Fluid Mech.*, 1983, **131**, 155.
52 B. Cichocki and B. U. Felderhof, *J. Chem. Phys.*, 1988, **89**, 3705.
53 M. P. Lettinga, M. A. M. J. van Zandvoort, C. M. van Kats and A. P. Philipse, *Langmuir*, 2000, **16**, 6156.
54 G. K. Batchelor, *J. Fluid Mech.*, 1982, **119**, 379.
55 A. J. Banchio, J. Bergenholtz and G. Nägele, *Phys. Rev. Lett.*, 1999, **82**, 1792.
56 G. H. Koenderink, S. Sacanna, C. Pathmamanoharan, M. Rasa and A. P. Philipse, *Langmuir*, 2001, **17**, 6086.
57 M. Watzlawek and G. Nägele, *Phys. Rev. E*, 1997, **56**, 1258.
58 F. Bitzer, T. Palberg and P. Leiderer, unpublished results.
59 E. Overbeck, S. Sinn and M. Watzlawek, *Phys. Rev. E*, 1999, **60**, 1936.
60 M. Doi, *J. Phys. (France)*, 1975, **36**, 607.
61 W. Kuhn and H. Kuhn, *Helv. Chim. Acta.*, 1945, **28**, 97.
62 D. H. Berry and W. B. Russel, *J. Fluid Mech.*, 1987, **180**, 475.
63 T. G. Mason and D. A. Weitz, *Phys. Rev. Lett.*, 1995, **74**, 1250.
64 M. J. Solomon and Q. Lu, *Curr. Opin. Colloid Interface Sci.*, 2001, **6**, 430.